IEEE Access
Multidisciplinary | Rapid Review | Open Access Journal

Received November 16, 2020, accepted November 30, 2020, date of publication December 9, 2020,
date of current version December 21, 2020.

Digital Object Identifier 10.1109/ACCESS.2020.3043462

Research on the Heading Control of Underwater Vehicle Under Hover Condition

FEIYAN MIN[1,2], FANGHONG YANG[1], GAO WANG[1], AND XINYU YE[2]
[1]College of Information Science and Technology, Jinan University, Guangzhou 510632, China
[2]Navigation Instruments Institute of Tianjin, China Shipbuilding Industry Corporation (CSIC), Jiujiang 332007, China

Corresponding authors: Gao Wang (twangg@jnu.edu.cn) and Xinyu Ye (xinyu.ye@foxmail.com)

This work was supported in part by the Key Laboratory Fund under Grant 6142002180408, and in part by the Pre-Research Fund of China under Grant 61400010206.

ABSTRACT A guidance and control algorithm for the heading control of a large underwater vehicle in hover state is proposed. The complexity of the flow field makes it difficult to build an accurate mathematical model for heading control under hover condition. Furthermore, the turning motion in the hover state causes additional vertical hydrodynamic and pitching moments which may affect the control performance of depth and pitching, and even bring safety problems. An H_∞ synthesis method is proposed, in which guidance weighting function is designed for the heading control constraints, sensitivity weighting function for the tracking performance requirements, and uncertainty weighting function for modeling error. Firstly, the hydrodynamic characteristics and constraints of hover and steering are analyzed, and the mathematical model is established. Secondly, based on the analysis of the affection of steering motion on depth and trim state, a control strategy is proposed to suppress interference by setting steering speed and limiting acceleration, which improves the safety of the control algorithm. And then, a H_∞ robust control algorithm based on three kinds of weighting function is designed. Finally, the method is simulated by using submarine model and validated by underwater vehicle experiment.The research in this article has potential application value for safety and low noise performance for the control of large underwater platform and manned submarines.

INDEX TERMS Hover, underwater vehicle, manned submarine, H_∞ robust control, guidance law.

I. INTRODUCTION

Hovering is a manipulation mode maintaining depth and attitude for underwater vehicle in zero speed or extreme-low speed state. The manipulation effectiveness of rudder under this mode is limited, and the control is mainly based on ballast tank and propeller. Hovering is a very important capability for autonomous underwater vehicles (AUV) and large underwater platform.

In the past few years, several hovering unmanned underwater vehicles have been developed. Hover manipulation extend the capabilities of underwater robots, allowing them to perform more complex tasks. These tasks, including underwater target identification, communications and underwater docking, which require the ability to hover at a fixed point. In particular, future underwater robots will replace humans to do most kinds of underwater work. Hover control is one of the most important underwater capabilities of future AUV. However hovering robots face many kinds of interference, such as the reaction force of manipulator motion and interference of environmental factors. In underwater missions, the robot must maintain its depth, direction and posture. Therefore, the robot must be able to complete the motion control of six degrees of freedom in the hover state, see [1].

On the other hand, hover manipulation is important manipulating means for large underwater vehicles, such as underwater platform [2] and submarine to achieve depth stability at zero speed in response to environmental changes in density, pressure and wave forces. Hover control will effectively support various military missions, such as missile launch, AUV deployment and recovery, underwater replenishment, etc., see [3], [4]. In case of emergency, the water in the hovering tank is discharged to reduce the weight of the submarine, which can effectively enhance the emergency rise capability. In addition, the main engine will be close and the radiation noise is very small under hovering condition, which is extremely beneficial for the submarine stealth performance.

The associate editor coordinating the review of this manuscript and approving it for publication was Jiajia Jiang.

Therefore, the research on the submarine hover control technology is also highly regarded.

Different hover devices are developed, which puts forward many requirements for the modeling and control problem of the hover system, see [5]. For small autonomous underwater vehicle (AUVs), the hover control is performed primarily by propellers that track the depth instruction while limiting the pitch angle. However, for large underwater vehicles such as manned submarines, the traditional hover control system is completed by hydraulic pumps and ballast tanks, and auxiliary thrusters is redundant, inevitably resulting in radiated noise. Ballast water tank specially designed for hovering, mainly located near the center of mass along the length of the submarine, see [6]. In addition, there are other novel methods of submarine hover depth control. Buck proposed a jet control system that controlled the response of four jet hover jets to offset the reaction forces of circulation, suction and missile, see [7].

In recent years, people have done a lot of researches on the hover depth control methods and algorithms of underwater vehicle. A low-cost, highly mobile underwater vehicle has introduced internal buoyancy and balance control mechanisms to enable it to hover and carry dynamic loads when performing a single task, see [8]. This underwater vehicle, named AMOUR (version 5), can achieve efficient motion without considering the size of the payload. In reference [9], aiming at the slight maneuver and slow time-varying characteristics of AUV in the hover process, speed feedback is introduced on the basis of position closed-loop control to realize fixed-point dynamic hover of AUV. In literature [10], a depth and trim control method for large AUV hover state is introduced, and the control device is a two-tank variable buoyancy system (VBS). Literature [11] proposes a decoupling control algorithm for autonomous underwater vehicle hovering near the surface. On the basis of decoupling of the system, two independent actuators (water tank) are used to control the depth and trim angle of AUV. The paper [12] discusses fault-tolerant control of a hovering underwater vehicle with four horizontal thrusters and two vertical thrusters. Besides, meaningful explorations have been carried out on AUV hover depth control, including hover motion modeling and simulation ([6], [13], [14], [15]), test platform construction ([16], [17]), high-performance control algorithm([7], [8]), etc.

In general, underwater vehicle control is usually decoupled into vertical (depth and trim) control subsystem and horizontal (heading and position) control subsystem. The work mentioned above mainly focuses on the control of vertical plane, i.e. depth and pitch control. However, there is little research on the heading and course control in hover state. With the development of research, it is found that the heading control in hover state is also very important. For underwater robots, the stability of hover heading and position is crucial to complete the underwater mission. And for underwater platform and submarine, it must be able to maintain and adjust its heading under the ocean current condition when hovering for tactical needs.

It is found that the depth and heading of the hover state are more susceptible than higher speed state to environmental interference due to the low maneuvering force. Therefore, the model uncertainty of hover state has a greater affection on the control performance and the robust control provides a considerable option.

The research [19] presents a formulated weighting function design method in mixed-sensitivity H_∞ control system. In the method, weighting functions can be readily determined from the analysis of AUV control objectives. And in [20], authors propose a new method to synthesize a structured controller for the heading control of Autonomous Underwater Vehicle (AUV) with two H_∞ constraints and two parametric uncertainties formulation. A robust adaptive fuzzy neural network control algorithm is proposed based on a generalized dynamic fuzzy neural network (GDFNN) and PID algorithm, for heading the control of the unmanned marine vehicle (UMV) in the presence of a complex environment disturbance [21].

The hovering heading control of underwater vehicle mainly faces several challenges:

(1) Horizontal motion (sway and yaw) in hover state will bring additional vertical hydrodynamic forces and pitching moments. These forces are not negligible relative to the hover depth control forces. The turning motion can cause the boyancy loss and negative trim, and it affects the hover depth control performance seriously, and even cause safety hazard. Therefore, the control coupling between vertical plane and horizontal plane in hover state must be carefully considered. The problem is particularly acute for large vehicle and submarines, see [18], [22].

(2) In our previous study [23], it was found that the complex flow field around underwater vehicle during turning motion under hover condition, which affected the operation efficiency of the propeller, and it was difficult to obtain accurate mathematical model, thus affecting the performance of the control algorithm.

(3) Hover is usually a low power and low noise manipulation mode for submarine. Therefore, the control strategy must be low power consumption and low manipulation frequency, see [24].

Aiming at the above problems, this article proposes a heading control algorithm based on robust H_∞ method. Firstly, the causes of ship buoyance loss and negative trim during steering are analyzed. It is found that limiting of steering acceleration and constant turning velocity can effectively suppress hydrodynamic affections. Secondly, a guidance law of constant steering rate is designed, which can effectively limit the turning rate and acceleration. And then, guidance law proposed is simplified as weighting function, tracking performance is described as sensitivity function and modeling error is modeled as uncertainty weighting function, and the design principle of these weighting function is researched based on robust tracking performance and robust stability.

For the last, the robust H_∞ control law implemented with the weighting functions.

The ultimate purpose of this article is to provide control algorithm and scheme for large underwater platform and submarine. Considering the feasibility and safety, the research is validated on AUV for the first phase. For this reason, a submarine model is used to simulate and verify the method, and an AUV is further used to validate the research. The method proposed in this article may plays an important role in the safe operation and low noise control of large underwater platform and submarine.

II. MATHEMATICAL MODEL AND MANIPULATION CONSTRAINTS FOR HOVER MOTION

The underwater vehicle can be modeled as a rigid body with six degrees of freedom, and its translational and rotational equations can be established according to Newton's laws. According to Fossen's scheme in [25], earth fixed reference frame $O\xi\eta\zeta$ and body reference frame $oxyz$ shafting are respectively established, as shown in Figure 1.

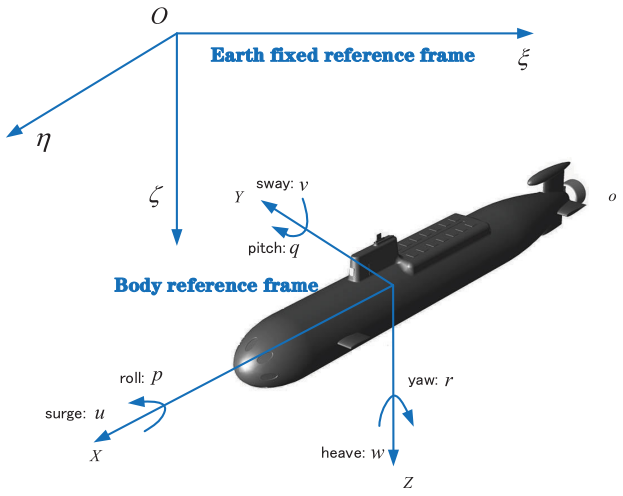

FIGURE 1. Reference frame of underwater vehicle.

The linear velocity of the vehicle in ox, oy, oz direction is u, v, w, the angular velocity is p, q, r, and the forces and torques are X, Y, Z and K, M, N, respectively. Then the dynamic and dynamic moment equations of the vehicle in the ox, oy, oz direction can be described as

$$\begin{cases} m[\dot{u}-vr+wq+z_G(pr+\dot{q})]=\sum X \\ m[\dot{v}-wp+ur+z_G(qr-\dot{p})]=\sum Y \\ m[\dot{w}-uq+vp-z_G(p^2+q^2)]=\sum Z \\ I_x\dot{p}+m[z_G(\dot{v}-wp+ur)]=\sum K \\ I_y\dot{(q)}+(I_x-I_z)rp+m(z_G(\dot{u}-vr+wq))=\sum M \\ I_z\dot{(r)}+(I_y-I_x)pq=\sum N \end{cases} \tag{1}$$

where I_x, I_y, and I_z are the moment of inertia in the x, y and z directions, respectively. m is the displacement and z_G is the position of center of gravity in z direction.

When the vehicle hovers underwater, its speed is approximately zero. Its depth is controlled by either a vertical propeller or a buoyancy adjustment tank. The main devices of heading control is the lateral thrusters installed at ship bow or stern.

Based on the above hypothesis, the dimensionless equation of the motion of hovering vertical plane can be obtained as follows:

$$\begin{cases} m[\dot{u}-vr+wq-x_G(q^2+r^2)-y_G\dot{r}+z_G\dot{q}] \\ \quad=\frac{1}{2}\rho L^3 X'_{\dot{u}}\dot{u}+\frac{1}{2}\rho L^2(X'_{uu}u^2+X'_{ww}w^2)+\frac{1}{2}\rho L^4 X'_{qq}q^2 \\ \quad+\frac{1}{2}\rho L^3 X'_{wq}wq+(W-B)\sin\theta+V_h\sin\theta \\ m[\dot{w}-uq+vp-z_Gq^2-x_G\dot{q}+y_Grq] \\ \quad=\frac{1}{2}\rho L^2(Z'_w uw+Z'_{vv}v^2+Z'_0 u^2)+\frac{1}{2}\rho L^4(Z'_{\dot{w}}\dot{w}+Z'_{\dot{q}}\dot{q}) \\ \quad+\frac{1}{2}\rho L^3 Z'_q uq+\frac{1}{2}\rho L^2 Z'_{ww}w^2+\frac{1}{2}\rho L^3 Z'_{vr}vr \\ \quad+(W-B)\cos\theta+V_h\cos\theta \\ (I_y\dot{q}-I_{xy}qr-r^2)-I_{yz}\dot{r}+m[z_g(\dot{u}-vr+wq)-x_G\dot{w}] \\ \quad=\frac{1}{2}L^5(M'_{\dot{w}}\dot{w}+M'_{\dot{q}}\dot{q}) \\ \quad+\frac{1}{2}\rho L^4(M'_q uq+M'_{ww}w^2+M'_{vr}vr) \\ \quad+\frac{1}{2}\rho L^3(M'_0 u+M'_w uw+M'_{vv}v^2)+Wz_G\cos\theta \\ \quad+Bx_B\cos\theta-Bz_B\sin\theta \\ \dot{\zeta}=-u\theta+w \\ \dot{\theta}=q \end{cases} \tag{2}$$

where ξ, η, ζ is the position coordinate in the earth fixed reference frame, ϕ, θ, ψ is the transverse roll angle, pitch angle, and yaw angle, respectively. W is the weight of the vehicle, B is its buoyancy, and V_h is the control variable of the hover ballast tank. x_G, y_G, z_G is the geometric position of the center of gravity, x_B, y_B, z_B is the geometric position of the buoyancy force, and X'_*, Y'_*, Z'_* is the hydrodynamic coefficients on surge, sway, heave direction, respectively.

Similarly, on the basis of the above hypothesis, the dimensionless equation of the submarine's zero speed horizontal motion can be obtained as follows:

$$\begin{cases} m[\dot{v}+ur-y_gr^2+z_gqr+x_g\dot{r}] \\ \quad=\frac{1}{2}\rho L^2 Y'_0 u^2+\frac{1}{2}\rho L^4(Y_{\dot{v}}\dot{v}+Y_{\dot{r}}\dot{r})+\frac{1}{2}\rho L^2 Z'_v uv \\ \quad+\frac{1}{2}\rho L^3 Z'_r ur+\frac{1}{2}\rho L^2 Z_{vv}v^2+Y_T T \\ I_z\dot{r}-I_{yz}\dot{q}+I_{xy}q^2+I_{xy}rq \\ \quad+m[x_g(\dot{v}+ur)-x_g(\dot{u}-uv+wq)] \\ \quad=\frac{1}{2}\rho L^5(N'_{\dot{v}}\dot{v}+N'_{\dot{r}}\dot{r})+\frac{1}{2}\rho L^3(N'_0 u^2+N'_v uv) \\ \quad\frac{1}{2}\rho L^4(N_r ur+N'_{vv}v^2)+N_T T \\ \dot{\psi}=r \end{cases} \tag{3}$$

where T is the thrust of side propeller, and it denotes the heading control capability under hover condition. The main

control device is propeller for the turning manipulation under hover condition. They are related to propeller diameter D_p, propeller speed n, inlet velocity Va, water density p, water viscosity coefficient v and gravitational acceleration g. The value of thrust T and torque Q can be computed with following equation [27]:

$$T = \rho n^2 D_p^4 f_1\left(\frac{Va}{nD_p}, \frac{nD_p^2}{v}, \frac{n^2D_p^2}{gD_p}\right) = \rho n^2 D_p^4 K_T \quad (4)$$

$$Q = \rho n^2 D_p^5 f_2\left(\frac{Va}{nD_p}, \frac{nD_p^2}{v}, \frac{n^2D_p^2}{gD_p}\right) = \rho n^2 D_p^5 K_Q \quad (5)$$

where f_1 and f_2 are nonlinear functions of propeller thrust and torque coefficient. The thrust coefficient and torque coefficient can be obtained by the open water test of the propeller. Another key parameter of the propeller is the efficiency factor:

$$\eta = \frac{TVa}{Qn2\pi} \quad (6)$$

The thruster's thrust coefficient K_T and torque coefficient K_Q are related to various factors, which are affected by factors such as water velocity, wake coefficient and thrust reduction coefficient, and the installation mode of thruster and ocean current environment.

The main constrains for hover heading control are discussed below. Simulation and experimental results show that the lateral thrusters can produce steering motion, sway velocity v as well as surge velocity w of a smaller magnitude. In addition, it is found that steering and lateral motion can also cause the change of hydrodynamic force in the vertical plane and the change of pitching moment, that is buoyance loss and negtive trim.

The main reason for the above problems is that large underwater vehicles tend to have asymmetrical configuration, and the horizontal movement will generate additional hydrodynamic force in the vertical plane, see Figure 2. As reflected in the mathematical model, item $Z'_{vr}, Z'_{vv}, M'_{vr}, M'_{vv}$ has a relatively large value, and evidence can be found in the literature [25], [26].

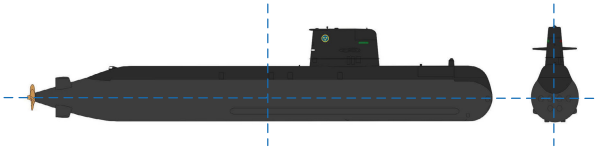

FIGURE 2. The shape asymmetry lead to the additional vertical hydrodynamic forces and moment during hover steering.

On the other hand, the depth manipulation ability under hover condition is weak, which makes the above problems more serious.

III. ALGORITHM OF HEADING CONTROL UNDER HOVER CONDITION

The control algorithm includes two aspects: depth control and heading control. In this research, we focus on the guidance and control law for heading steering to avoid the influence between the two aspects.

A. HOVER DEPTH CONTROL LAW

For the depth control algorithm, the depth deviation and depth rate of the vehicle is used to synthesize the control force of Z direction and then convert to the command of ballast tank or vertical propeller. In our research, a depth controller is designed by referring to the method in literature [28], and its form is:

$$\delta_V = k_{\dot\zeta}\dot\zeta^* + k_{\dot\zeta|\dot\zeta|}\dot\zeta^*|\dot\zeta^*| + k_p(\dot\zeta^* - \dot\zeta) + k_I(\zeta^* - \zeta) \quad (7)$$

where, $\dot\zeta^*, \zeta^*, \dot\zeta, \zeta$ is the reference depth rate, reference depth, actual depth rate and actual depth respectively. And the calculation method is listed below. The above equation is composed of four terms. The first two terms represent the feedforward compensation terms of the hydrodynamic force in the process depth adjustment, $k_{\dot\zeta}$ and $k_{\dot\zeta|\dot\zeta|}$ is corresponding hydrodynamic coefficient. The last two terms are typical PI controllers.

We select the characteristic equation as

$$s^2 + 2\sigma s + \sigma^2 + \omega_n^2 = 0 \quad (8)$$

And calculate the control parameters:

$$k_p = 2m\sigma - k_{\dot\zeta} - 2k_{\dot\zeta|\dot\zeta|}|\dot\zeta^*| \quad (9)$$

$$k_I = m(\sigma^2 + \omega_n^2) \quad (10)$$

where m is the displacement of submarine, the reference depth rate can be calculated with:

$$\dot\zeta^* = -\lambda(\zeta - \zeta^*) \quad (11)$$

$$\zeta^* = \int \dot\zeta^* dt \quad (12)$$

λ is the guidance rate parameter, the choice of $\lambda, \sigma, \omega_n$ is referred to literature [28].

Controller (7) calculates the vertical force for the depth control. For AUV equipped with vertical thrusters, the control force is then converted to the balance to each thruster instruction.

For an AUV or submarine with ballast tanks, a nonlinear conversion of relay characteristic is required. The relation curve of input and output of relay characteristic is shown in Figure 3, the instruction of drainage and injection can be generated. In the figure, the abscissa is the instruction of the controller to discharge water, and the ordinate is the instruction to discharge water, 1 is the drainage, -1 is the injection, and 0 is the closure of the pipeline.

B. GUIDANCE LAW FOR HEADING CONTROL

The guidance law is used to generate the desired heading angle and steering rate aimed to limit the variation in weight and pitch during steering motion and to accommodate the limitation of the vehicle's steering capability (propeller output power). The guidance law is particularly important for large vehicle, due to the weak steering force under hovering

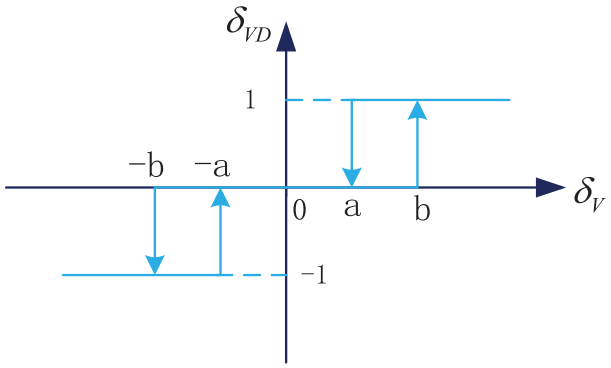

FIGURE 3. Command principle of ballast tank drainage and injection.

condition. The guidance law is also considered noise radiation and other restrictions.

The input of the guidance algorithm is the target heading angle, and the output includes real-time heading instruction and steering speed instruction. The algorithm consists of two loops. The inner loop is the steering speed planning loop, which limits the acceleration of steering. The outer loop is the heading angle planning loop, which limits the steering speed, and the setting steering speed can be specified in the limiting module.

The principle of the guidance law is shown in Figure 4.

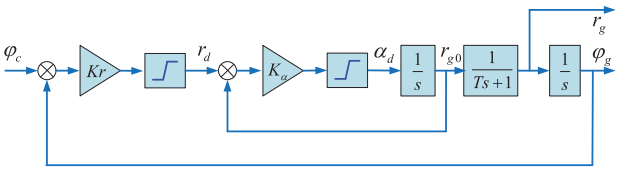

FIGURE 4. Principle of guidance law for heading control.

The input variables include target heading φ_c, command steering rate (or maximum steering rate) r_c, and maximum steering acceleration α_c. The intermediate variables for internal calculation include: internal instruction velocity r_d, internal instruction acceleration α_d, initial guidance velocity r_{g0}, guidance velocity r_g, and guidance heading φ_g.

The command steering speed r_c is used to accommodate the limitation of buoyance loss and negtive trim, and can be set by user; Maximum steering acceleration α_c is used to accommodate the propeller's power output limits, and it can be calculated with fluid mechanics dynamic.

The guidance process is described as follows:

Initialize the intermediate variablesf $r_d = 0$, $\alpha_d = 0$, $r_{g0} = 0$, $r_g = 0$ and $\varphi_g = \varphi$. The guidance heading is the current actual heading, and other intermediate variables are set to zero.

Calculate the internal command speed

$$r_d = K_r(\varphi_c - \varphi_g) \tag{13}$$

if $|r_d| > r_c$, limit the internal command heading speed:

$$r_d = sign(r_d) * r_c \tag{14}$$

Calculate the internal command of heading acceleration

$$\alpha_d = K_\alpha(r_d - r_{g0}) \tag{15}$$

if $|\alpha_d| > \alpha_c$, limit the internal command speed:

$$\alpha_d = sign(\alpha_d)\alpha_c \tag{16}$$

Then we can calculate guide velocity with

$$\begin{cases} \dot{r}_{g0} = \alpha_d \\ \dot{r}_g = K_g(r_{g0} - r_g) \\ \dot{\varphi}_g = r_g \end{cases} \tag{17}$$

where K_r, K_α, K_g ss the positive coefficient used to adjust the dynamic characteristics of the start and end stages of the guidance.

Finally, the guidance heading φ_g and speed r_g can be obtained by integrating the above three formulas.

C. HEADING CONTROL LAW

The propeller is the main device for the hover heading control of underwater vehicle, and its mathematical model is shown in (4) (5). The parameters that affect the performance of the propeller include water velocity, wake coefficient and thrust reduction coefficient, which make it difficult to obtain an accurate mathematical model.

For this reason, we use robust H_∞ method to synthesize the hover heading control algorithm.

The regulation schema is shown in Figure 5. ϕ_c is the reference heading angle and $W(s)$ is the weighting function of the guidance law. $W_S(s)$ is the weighted function of tracking error e, which reflects the suppression ability to disturbance d of the closed-loop system. $W_R(s)$ is the weighted function of the control inputs u, and it also reflects the range of uncertainty of the model. z_1, z_2 is the output of the weighted function. $D(s)$ is the model for disturbance, and $G(s)$ is the characteristic of steering dynamic of AUV in hovering state, and the nominal transfer function is as follows:

$$G(s) = \frac{q_1 s + q_0}{p_2 s^2 + p_1 s + p_0} \tag{18}$$

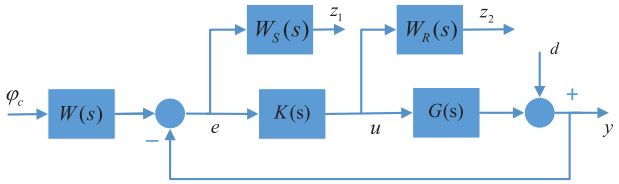

FIGURE 5. Regulation scheme with weighting functions for control law.

where p_0, p_1, p_2 and q_0, q_1 is uncertain parameter with a certain range and is related to sway velocity v of the vehicle. The nominal model can be obtained by simplifying (3) due to the independence of horizontal and vertical motion. The value of $u, q, \dot{u}, \dot{q}$ is set to zero, and v is set to a small enough value, then the transfer function between Ψ and T can be built. For the submarine model, The value of v is usually extremely

small, and equation (18) can be reduced to the second-order model.

In previous research [23], we found that additive uncertainty was suitable for describing steering dynamic in hover state.

The control model considering perturbation and uncertainty is shown in the figure, and the tracking error can be expressed as

$$e = S(I + \Delta R)^{-1}(r - d) \tag{19}$$

where, Δ is the additional uncertainty model, and $S = [I + G(s)K(s)]^{-1}$ and $R = K[I + G(s)K(s)]^{-1}$.

For the current control requirements, the weighting function is selected under the following considerations: (1) response speed and control accuracy of the vehicle open loop control system; (2) the modeling uncertainty, especially the model of lateral propeller. And we get the H_∞ control problem:

$$\begin{cases} \|W_S(s) \cdot S(s)\|_\infty < \gamma \\ \|W_R(s) \cdot R(s)\|_\infty < \gamma \end{cases} \tag{20}$$

D. WEIGHT FUNCTION DESIGN AND STABILITY ANALYSIS

According to the tracking performance and stability requirement, the weighting functions are iteratively design as follows.

Considering the tracking error e caused by disturbance d, for the nominal model($\Delta = 0$, $r = 0$), we have $e = -SDv$, as it shows in Figure 6. To suppress the disturbance, let

$$W_S(s) = w_1(s)I \tag{21}$$

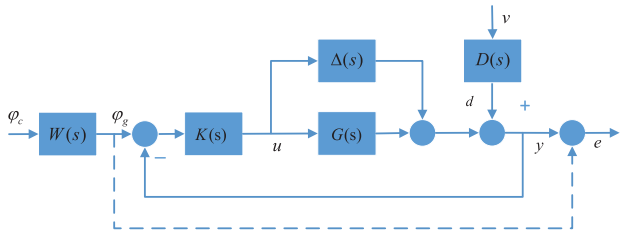

FIGURE 6. Control diagram considering disturbance and uncertainties model.

where $|w_1(j\omega)| \geq \bar{\sigma}[D(j\omega)]$ at all frequencies $\omega \in (0, \infty)$. So the relationship holds

$$\bar{\sigma}[W_S(j\omega)S(j\omega)] = |w_1(j\omega)|\bar{\sigma}[S(j\omega)] \geq \bar{\sigma}[S(j\omega)D(j\omega)] \tag{22}$$

and it follows

$$\|W_s(s)S(s)\|_\infty \geq \|S(s)D(s)\|_\infty \tag{23}$$

And

$$\|e\|_2 = \|S(s)D(s)v\|_2 \leq \|S(s)D(s)\|_\infty \|v\|_2 < \gamma\|v\|_2 \tag{24}$$

Therefore, it can suppress the affection of disturbance by design $W_S(s)$ with equation (21).

Therefore, the form of the weighting functions are

$$W_S = \frac{s/M + \omega_c}{s + \omega_c A} \; W_R = k \tag{25}$$

where A is the maximum steady accuracy requirement, M is the peak of sensitivity, and ω_c is the prospective bandwidth.

Then considering the robust stability under model uncertainty Δ, let

$$W_R(s) = w_2(s)I \tag{26}$$

where $|w_2(j\omega)| \geq \gamma\bar{\sigma}[\Delta(j\omega)]$ at all frequencies $\omega \in (0, \infty)$. Similarly, we get the relationship

$$\bar{\sigma}[W_R(j\omega)R(j\omega)] = |w_2(j\omega)|\bar{\sigma}[R(j\omega)] \geq \gamma\bar{\sigma}[R(j\omega)\Delta(j\omega)] \tag{27}$$

$$\|W_R(s)R(s)\|_\infty \geq \gamma\|R(s)\Delta(s)\|_\infty \tag{28}$$

And it follows with equation (20)

$$\|\Delta(s)R(s)\| < 1 \tag{29}$$

Then the small gain theorem is satisfied, and the closed-loop system is stable to the model uncertainty Δ by design $W_R(s)$ with equation (25).

In addition, it is desired that $\bar{\sigma}[G(j\omega)K(j\omega)] \gg 1$ in the low frequency band in order to improve the tracking accuracy, and it follows $R(s) \approx G^{-1}(s)$, then we get

$$\|W_R(s)\|_\infty < \gamma\|G(s)\|_\infty \tag{30}$$

and we get additional design constraints

$$|w_2(j\omega)| < \gamma\bar{\sigma}[G(j\omega)] \tag{31}$$

IV. SIMULATION WITH SUBMARINE MODEL

This part uses a submarine model [26] to verify the proposed algorithm. The submarine discharges 2,352 tons and is 67 meters long. In order to carry out the simulation experiment, the submarine maintains the hover state at extremely low speed, and the lateral thrust and torque are applied to the stern of the submarine to control the heading angle of submarine.

Firstly, the forward control characteristics of the model is linearized under the condition of fixed depth of hovering without speed ($u = 0, v = 0, w = 0, p = 0, q = 0$), and the transfer function from the turning thrust to the heading angle is obtained:

$$G_{\phi T}(s) = \frac{-8.1e - 6}{s^2 + 2.2e - 5s} \tag{32}$$

In the guidance algorithm design, the range of r_c is [0.1, 0.3] $^o/s$, and the selection of α_c is 0.01 $^o/s^2$.The weight function selected for the controller is:

$$\begin{cases} W(s) = \dfrac{5s + 1}{100\,s + 1} \\ W_S(s) = \dfrac{20s + 0.4}{20s + 0.002} \\ W_R(s) = 2e - 4 \end{cases} \tag{33}$$

Matlab mixsyn function is used to process the above control object and weight function, and the generated controller form is

$$K(s) = \frac{1447s^2 + 24.13s + 5.30e - 4}{s^3 + 2.69e - 1s^2 + 2.77e - 3s + 2.74e - 7} \quad (34)$$

The result robust performance $\gamma = 0.5$.

A. SIMULATION 1: SINGLE PROPELLER MODE WITH SETTING TURNING SPEED 0.1 DEGREES PER SECOND

The first experiment is to simulate a relatively slow steering conditions. Fig 7, fig 8, fig 9 and fig 10 show the simulation results under the condition that the initial ballast weight of the ship is 1.5 tons, the heading change is 150 degrees and the steering speed is 0.1 degrees/second.

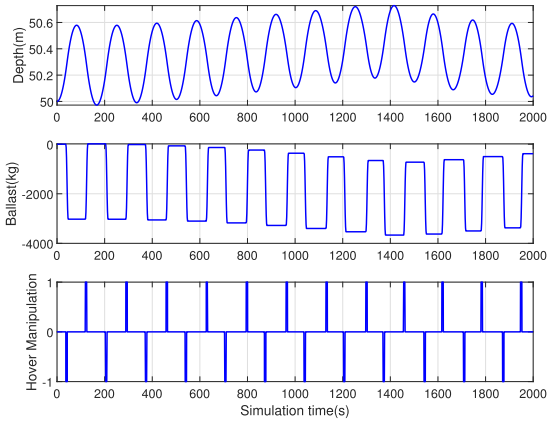

FIGURE 7. Hover depth and ballast variable in simulation 1.

We can see that the heading controller and the depth controller work in sync. During the control process, the depth control precision is within 0.7 meters and the trim angle is kept within 0.4 degrees. The performance of the depth control algorithm, such as the number of water drainage and injection, are not significantly affected by the steering process. The related performance is similar with heading keeping process, see Figure 7.

For the most part, the steering rate keeps $0.1^o/s$. No obvious deviation in pitch angle. The algorithm obtains good control performance, see figure 8. The value of hover manipulation refers to water injection and drainage, that is, 1 represents water injection, -1 represents drainage, and 0 represents the closure of the hover tank, according to the principle in Figure 3.

The Figure 9 shows the linear velocity during the hover turning.It can be seen that steering causes a small range of variations in speed. Obviously, these small speeds are within the control error of the submarine and do not affect stability. The Figure 10 shows the rotation speed and power of the stern side thruster. The power is higher during the starting and accelerating stage, while it remains basically unchanged afterwards, and this control strategy is helpful to maintain attitude stability.

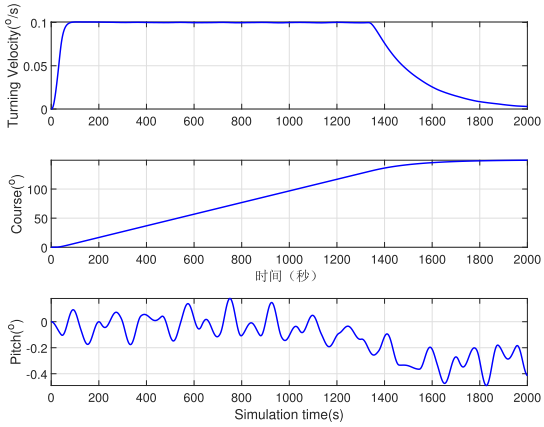

FIGURE 8. Hover course and pitch variable in simulation 1.

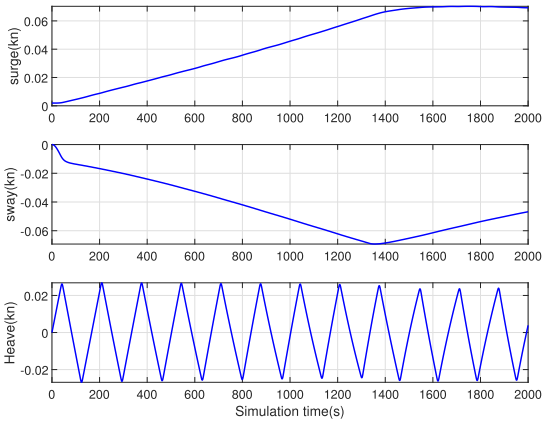

FIGURE 9. Linear velocity relevant variable in simulation 1.

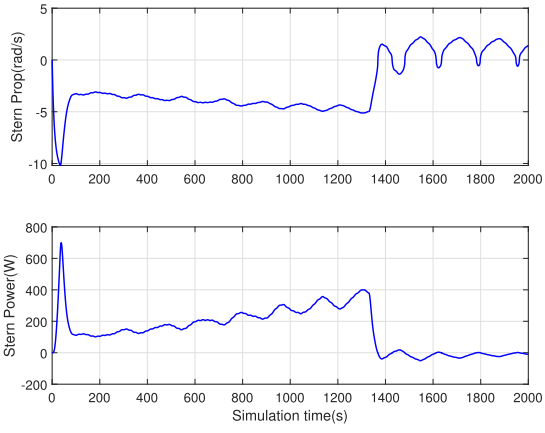

FIGURE 10. Propeller relevant variable in simulation 1.

In summary, the depth control performance is not affected by the heading change and manipulation in this experiment, the closed-loop control system in the whole motion process is stable, and the tracking accuracy of course instruction and steering speed instruction is considerably high.

B. SIMULATION 2: SINGLE PROPELLER MODE WITH SETTING TURNING SPEED 0.3 DEGREES PER SECOND

For the second experiment, a relatively fast steering condition is simulated.

Figure 11, 12, 13 and 14 shows the simulation results under the condition of initial unevenness measurement of 1.5 tons weight, 180 degrees steering and 0.3 degrees/second steering speed. We can see that the heading controller and the depth controller work in sync.

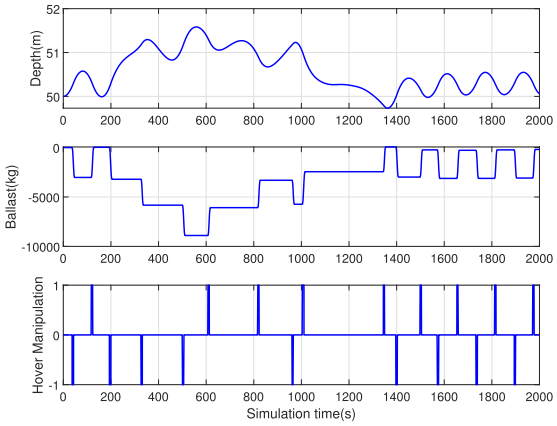

FIGURE 11. Hover depth and ballast variable in simulation 2.

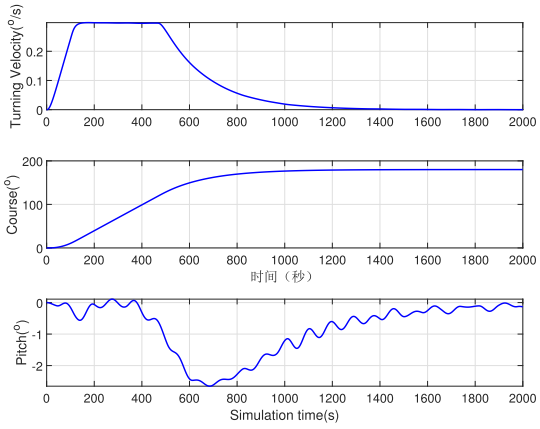

FIGURE 12. Hover course and pitch variable in simulation 2.

There is much difference in control performance of simulation 2 from simulation 1.

In the heading steering, there is obvious buoyance loss and trim deviation, which disappeared after the process. And that's the reason why depth and ballast increase while turning, as it shows in Figure 11. This is due to the fact that the steering process changes the dynamic buoyancy and pitching moment of the submarine, the faster the steering acceleration, the greater the effect.

That is one of the important reasons for the limited steering acceleration. In the control process, the control performance of depth and pitch get worse at start phase compared to simulation 1. The depth control precision is within 1.4 meters

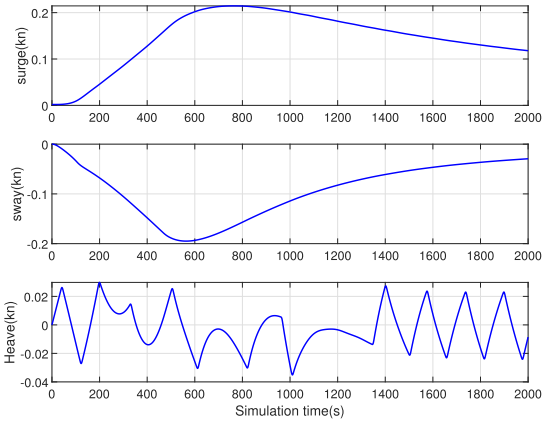

FIGURE 13. Linear velocity relevant variable in simulation 2.

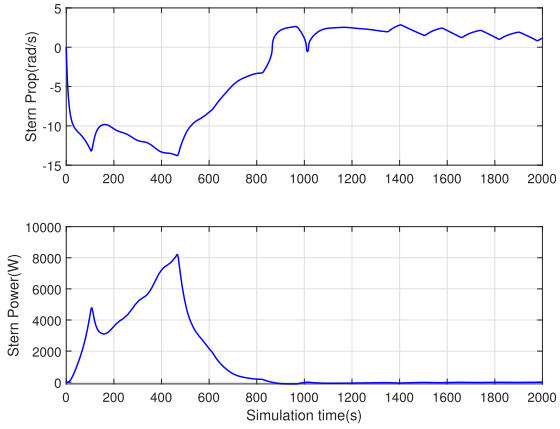

FIGURE 14. Propeller relevant variable in simulation 2.

and the trim angle is kept within 2.5 degrees. This deviation is acceptable for subs, but larger deviation must be avoid.

On the other hand, the heading control is not affected by the depth change, the closed-loop control system is stable during the latter motion process, and the tracking accuracy of course instruction and steering speed instruction is high.

Besides, the performance of the depth control algorithms, such as the number of water drainage and injection, are obviously affected by the steering process, see Figure 11. On the other hand, the characteristic of linear velocity and propeller power are similar to those in simulation 1, as it shown in Figure 13.

From the view of maneuverability and safety of submarine (e.g, the pitch angle must be below 5 degrees), the result is acceptable. But greater buoyance loss and pitch angle must be forbidden. That means the turning speed must be constant and acceleration must be limited in hover state.

V. VALIDATION WITH AUV

The ultimate goal of this study is to apply it to large underwater platform and submarine. However, considering the feasibility and security of the experiment, this research is validated on AUV in the first phase.

The AUV is 2200 mm long and the displacement is 68 kg, as shown in Figure 15. The control device contains

FIGURE 15. The AUV used for the validation of control algorithm.

two horizontal thrusters and two vertical thrusters, which are placed in the bow and stern respectively. In the experiment, the depth and pitch is stabilized by the vertical propeller AUV. And the heading control of AUV was achieved with horizontal propeller, which is used to verify the proposed guidance algorithm and control algorithm. The mathematical model of heading movement in researched condition is further simplified as follows:

$$\begin{cases} m_y\dot{v} = Y_v v + Y_r r + (1-t)T \\ I_z\dot{r} = N_v v + N_r r + (1-t)lT \\ \dot{\varphi} = r \end{cases} \tag{35}$$

where $T = K_t n^2$ is the thrust for heading control,l is the distance from the center of mass. The simplified form of transfer function can be obtained based on above model

$$G(s) = \frac{m_y l s + (N_v - l Y_v)}{m I_z s^2 + (-Y_v I_z - m_y N_r)s + (Y_v N_r - Y_r N_v)} \tag{36}$$

Due to the influence of water velocity, wake coefficient and thrust reduction coefficient, it is difficult to obtain accurate mathematical model. In our previous study, CFD calculation and parameter identification were used to obtain the parameters [23]. It was found that there were obvious differences in calculated parameters within different experimental samples. The CFD calculation parameters, identified parameters of bow propeller experiment and stern propeller experiment are shown in Table 1 respectively, and the corresponding frequency characteristics is shown in Figure 16.

TABLE 1. Parameters for steering model under hover condition.

Parameters	CFD caculation	Bow propeller experiment	Stern propeller experiment
Y_v	-1.009	-0.4668	-0.2244
Y_r	0.0940	0.1141	0.1023
N_v	-1.1433	-0.4707	-0.6152
N_r	-0.1661	-0.1162	-0.1366
t	0.25	0.29	0.24

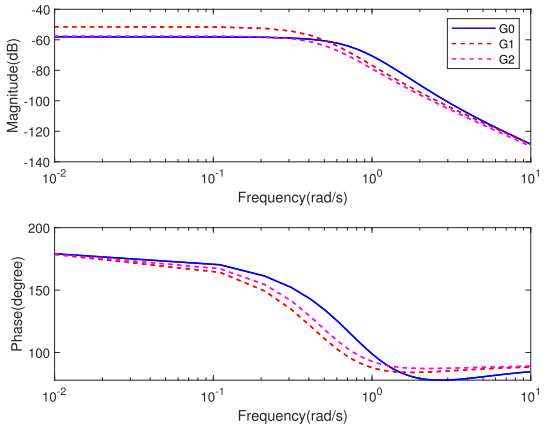

FIGURE 16. Bode diagram under different hydraulic parameters.

For the guidance law, the command steering rate r_c is set as 7 $^o/s$, and the steering acceleration limit α_c is 1.5 $^o/s^2$. There are several nonlinear components in the guidance rate, and the spectrum characteristics can be obtained with the linear analysis tool of MATLAB. In the controller design, approximate first-order weighted function $W(s)$is used to replace the guidance component, as shown in the figure 17.

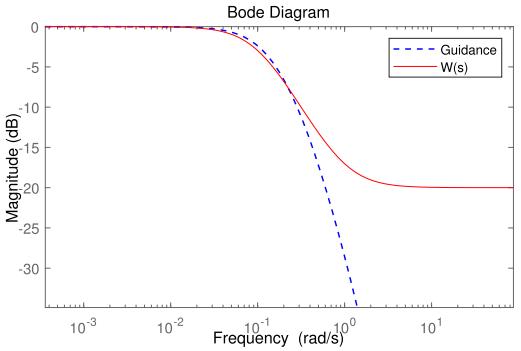

FIGURE 17. Spectral characteristics and weighting function of guidance law.

Through analysis, CFD calculation parameters in Table 1 are selected as nominal parameters, so the corresponding model is:

$$G(s) = \frac{35.7s + 8.68}{2244s^2 + 2907s + 1470} \tag{37}$$

The range of model uncertainty is also determined with the parameters in table 1, and the amplitude characteristics of $G_0 - G_1$, $G_0 - G_2$ and $G_0 - G_3$ are calculated respectively, as shown in Figure 18. It can be seen that the additive uncertainty model is approximately constant in the low frequency band. Based on this features, the weighted function W_R is selected as a constant value, and its range is $\|\Delta G(s)\|_\infty < W_R < \|G(s)\|_\infty$, that is $0.0001 < W_R < 0.013$.

For weighting function WS,the maximum steady accuracy requirement A_e is 0.01, the peak of sensitivity M_s is 1, the proceptive bandwidth of closedloop ω_c is 0.5.

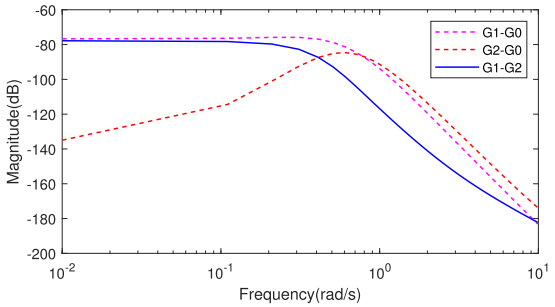

FIGURE 18. The range of model uncertainty ΔG.

The weighting functions are iteratively designed as follows

$$\begin{cases} W(s) = \dfrac{s+1}{10\,s+1} \\ W_S(s) = \dfrac{s+0.5}{s+0.05} \\ W_R(s) = 0.001 \end{cases} \tag{38}$$

Controller parameters are synthesized with Matlab Robust Control Toolbox. The final robust performance $\gamma = 0.501$, and the H_∞ controller designed is

$$K(s) = \frac{1400s^3 + 2320s^2 + 1573s + 331.8}{s^4 + 19.9s^3 + 42.7s^2 + 6.06s + 0.2} \tag{39}$$

The frequency response graph of $S(s)$, $S(s)K(s)$, $\gamma/W_S(s)$ and $\gamma/W_R(s)$ is shown in figure 19.

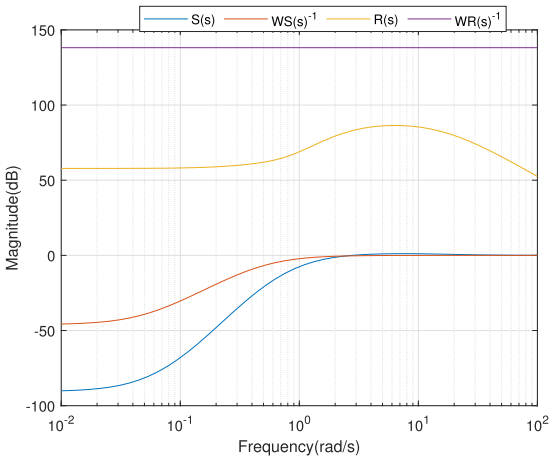

FIGURE 19. The spectrum of the weighting function.

During the experiment, INS and doppler log were used to record the AUV state. Figure 20 shows the attitude and pitch angle in the steering process. AUV completed 300 degree steering within 50 seconds. It is stable at other steering stages, and there is no excessive steering speed or acceleration. However, there is a large deviation at the end stage of the camber steering ($60s \sim 75s$), which may be due to a large tracking deviation.

During the steering process, the angular velocity of the three directions is shown in Figure 21. At the beginning of steering, the turning velocity rises to $-7\ ^o/s$, and then

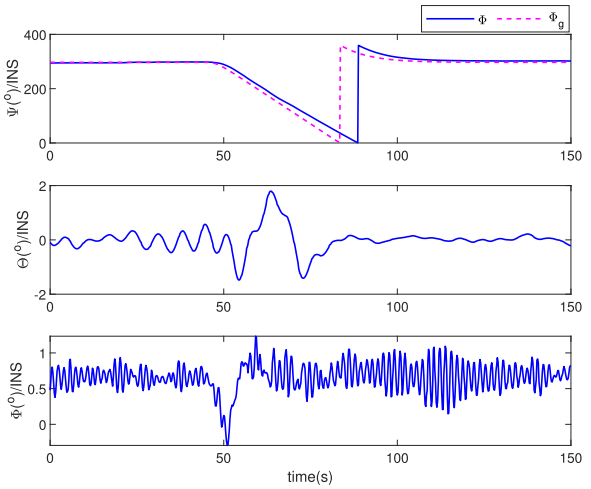

FIGURE 20. Course and attitude of AUV during experiment with proposed control law.

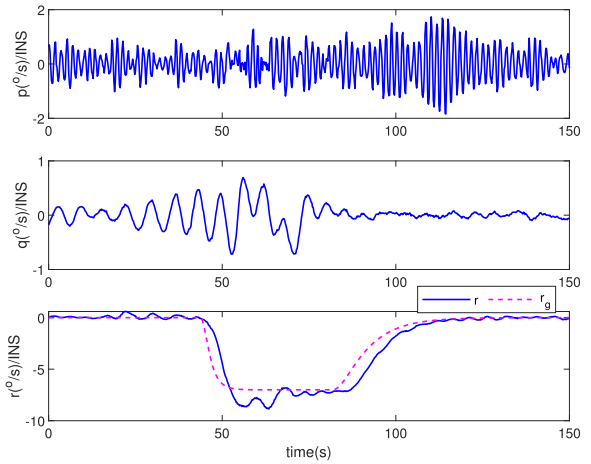

FIGURE 21. Angular velocity of AUV during experiment with proposed control law.

fluctuates around this value until the end of the steering process, thus realizing the control requirements proposed by the guidance algorithm.

The process of linear velocity and depth change is shown in Figure 22. It can be seen that at the beginning of steering, both speed and depth has obvious deviation, but remains near the set value in the subsequent process, which is consistent with the state change process of simulation results of submarine. The propeller speed during this process is shown in Figure 23, large fluctuations occur during the turning process, while other moments are more stable.

On the other hand, the standard PD controller is also designed to carry out the hover steering experiment, which do not include guidance law to limit the steering speed and acceleration in the algorithm. The form of control law is

$$K(s) = \frac{1000s + 30}{0.1s + 1} \tag{40}$$

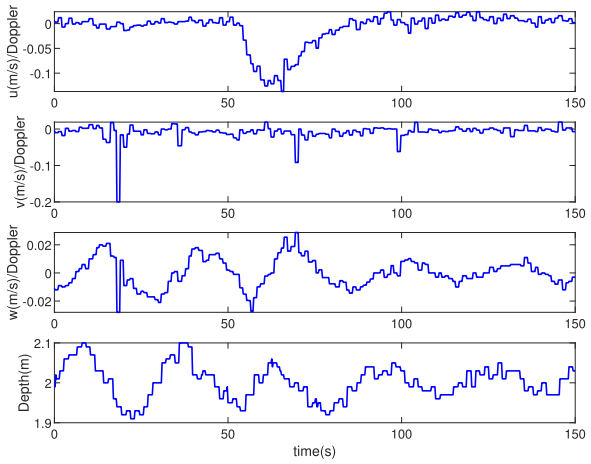

FIGURE 22. Linear velocity and depth of AUV during experiment with proposed control law.

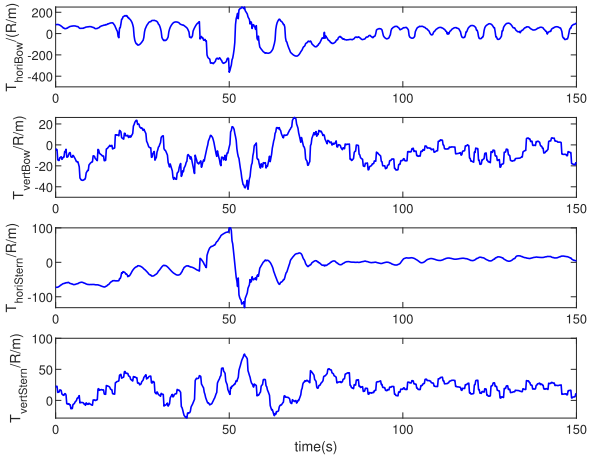

FIGURE 23. Propeller variable of AUV during experiment with proposed control law.

The results of the steering experiment are shown in the Figure 24-27. It can be seen that the turning rate and pitch angle fluctuated in a large range, with the maximum steering rate of 11 degrees at the beginning and 0 to 4 degrees in the subsequent stages. Depth control performance deteriorates due to fluctuations in speed and pitch. These deviations and fluctuations are acceptable for small AUVs but must be overcome for large submersibles.

The PD method is inferior to the robust method in terms of safety and low-noisy manipulation.

As we can see, the guidance and control algorithm proposed can realize the AUV heading control in the hover state. The algorithm can control heading speed to set value, thereby limiting the affection on the vertical control performance while heading steering, and then avoid frequent manipulation of vertical plane. Predictably, when the heading acceleration is set to small enough, depth and pitch angle of deviation at initial point will be cleared up.

In summary, our control algorithm is expected to improve hover heading control performance. The proposed approach

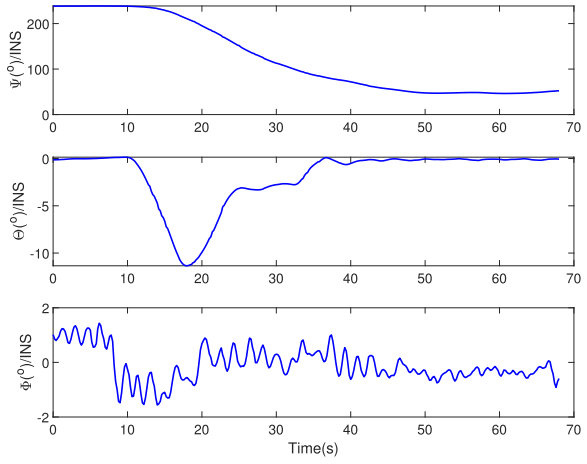

FIGURE 24. Course and attitude of AUV during comparative experiment.

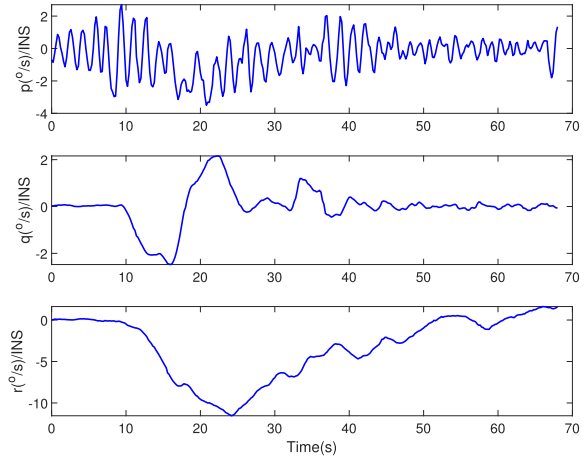

FIGURE 25. Angular velocity of AUV during comparative experiment.

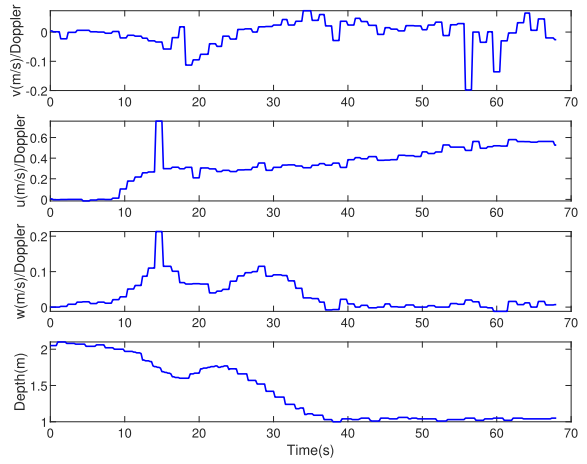

FIGURE 26. Linear velocity and depth of AUV during comparative experiment.

can achieve the decoupling of hover depth and heading control, and then effectively reduce the frequency of manipulation, for the underwater vehicle, especially for the low noise operation of submarine.

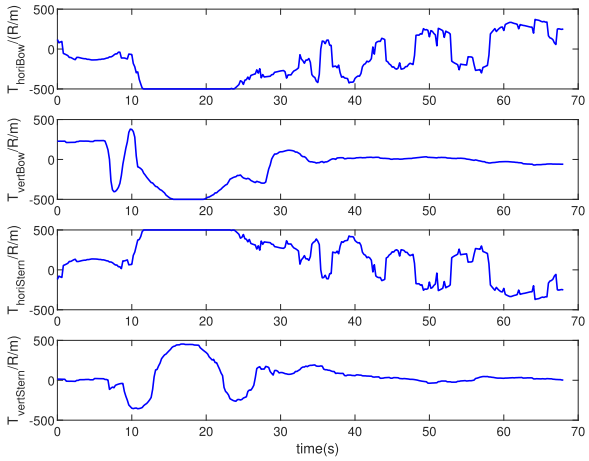

FIGURE 27. Propeller variable of AUV during comparative experiment.

VI. CONCLUSION

In this work, we present a guidance and control law for the heading steering of underwater vehicle in hovering state. The research is validated by simulation and experiment result. The conclusions may be summarized as follows:

(i) The control performance of steering under hover state may affected by the coupling interference between vertical and horizontal control which includes two aspects, the vehicle buoyancy loss and negative pitch. In order to avoid excessive repeated injection and drainage induced by the coupling interference, it is recommended to use constant turning speed law during steering. This is because the buoyance variation of the subs is mainly dependent on the steering speed.

(ii) The proposed guidance law can effectively limit steering speed and steering acceleration, thus limiting subs buoyancy loss and negative trim. And in this way, the heading control manipulation will not affect the performance of the depth control. The flow field characteristics under hover steering condition are complicated and the propeller model has complex uncertainty. Robust control law based on mixed sensitivity can effectively limit the influence of model uncertainty.

(iii) This article proposes a H_∞ design method, which uses the feedforward weighting function $W(s)$ to describe the guidance law, the sensitivity weighting function $W_S(s)$ for the tracking performance requirements, and the weighting function $W_R(s)$ for the uncertainty of the model. This method can effectively realize the hover-steering control of a large underwater vehicle.

In the future work, the analysis method of uncertainty model of large underwater platform and submarine under hover condition will be researched, and proposed guidance and control law will be implemented.

REFERENCES

[1] S. Jin, J. Kim, J. Kim, and T. Seo, "Hovering underwater robotic platform with four tilting thrusters," in *Proc. IEEE/ASME Int. Conf. Adv. Intell. Mechatronics*, Jul. 2014, pp. 1547–1551.

[2] A. L. Forrest, B. E. Laval, D. S. S. Lim, D. R. Williams, A. C. Trembanis, M. M. Marinova, R. Shepard, A. L. Brady, G. F. Slater, M. L. Gernhardt, and C. P. McKay, "Performance evaluation of underwater platforms in the context of space exploration," *Planet. Space Sci.*, vol. 58, no. 4, pp. 706–716, Mar. 2010.

[3] T. Hardy and G. Barlow, "Unmanned underwater vehicle (UUV) deployment and retrieval considerations for submarines," in *Proc. 9th Int. Naval Eng. Conf. Exhib.*, Hamburg, Germany, 2008, pp. 1–15.

[4] E. A. M. Conesa and D. Oakley, "Naval architecture challenges for integration of unmanned underwater vehicles in submarines," in *Proc. 1st Submar. Inst. Aust. Technol. Eng. Conf.*, Adelaide, SA, Australia, 2011, pp. 1–8.

[5] Y. Chen, G. Wang, G. Xu, W. Zhang, and W. Wang, "Hovering control of submarine based on L1 adaptive theory via ballast tanks," *Int. J. Adv. Robot. Syst.*, vol. 14, no. 4, pp. 1–10, Jul. 2017.

[6] Y. Chen, G. Xu, G. Wang, G. Liu, and W. Zhang, "Modelling and simulation for underwater hovering control based on ballast tank," in *Proc. IEEE Int. Conf. Underwater Syst. Technol., Theory Appl. (USYS)*, Penang, Malaysia, Dec. 2016, pp. 218–223.

[7] H. Runan and D. Ning, "AUV vertical plane control based on improved PID neural network algorithm," *J. Syst. Simul.*, vol. 32, no. 2, pp. 85–91, Feb. 2020.

[8] I. Vasilescu, C. Detweiler, M. Doniec, D. Gurdan, S. Sosnowski, J. Stumpf, and D. Rus, "AMOUR V: A hovering energy efficient underwater robot capable of dynamic payloads," *Int. J. Robot. Res.*, vol. 29, no. 5, pp. 547–570, Apr. 2010.

[9] M. A. Yan-Tong *et al.*, "AUV horizontal hover control based on position-speed closed loop," *Control Eng. China*, vol. 26, no. 10, pp. 1180–1184, Oct. 2019.

[10] S. Tangirala and J. Dzielski, "A variable buoyancy control system for a large AUV," *IEEE J. Ocean. Eng.*, vol. 32, no. 4, pp. 762–771, Oct. 2007.

[11] Y.-P. Yang, Y.-X. Zhao, Y.-L. Hao, and H.-Y. Du, "Decoupling control system for AUV hovering nearsurface," *Syst. Eng. Electron.*, vol. 34, no. 3, pp. 572–577, 2012.

[12] J.-K. Choi and H. Kondo, "On fault-tolerant control of a hovering AUV with four horizontal and two vertical thrusters," in *Proc. Oceans IEEE Sydney*, May 2010, pp. 1–6.

[13] F. Roberto *et al.*, "Modelling and control of blowing-venting operations in manned submarines," *J. Control Eng. Technol.*, vol. 4, no. 1, pp. 37–49, 2011.

[14] Y. Yang and Y. Hao, "Adaptive fuzzy modeling of hovering submarine based on on-line clustering," in *Proc. 7th Int. Conf. Fuzzy Syst. Knowl. Discovery*, Yantai, China, Aug. 2010, pp. 86–90.

[15] X. Ying and X. Jian, "Simulation of submarine hovering based on PID control," in *Proc. 2nd Int. Asia Conf. Informat. Control, Autom. Robot. (CAR)*, Wuhan, China, Mar. 2010, pp. 224–226.

[16] J. H. Li, S.-K. Park, S.-S. Oh, J.-H. Suh, G.-H. Yoon, and M.-S. Beak, "Development of a hovering-type intelligent autonomous underwater vehicle," in *Autonomous Underwater Vehicles*, N. A. Cruz, Ed. Rijeka, Croatia: InTech, 2011.

[17] Y. Xia, G. Xu, K. Xu, Y. Chen, X. Xiang, and Z. Ji, "Dynamics and control of underwater tension leg platform for diving and leveling," *Ocean Eng.*, vol. 109, pp. 454–478, Nov. 2015.

[18] J. R. Buck, "Pure fluidic control system for submarine hover during missile launching," *Nav. Eng. J.*, vol. 80, no. 5, pp. 759–766, Oct. 1968.

[19] L. Jing-Yang *et al.*, "Design of H_∞ control system for autonomous underwater vehicles," *Ocean Eng.*, vol. 26, no. 3, pp. 70–77, Aug. 2008.

[20] D. Monnet, J. Ninin, and C. B, "A global optimization approach to H_∞ synthesis with parametric uncertainties applied to AUV control," *IFAC-PapersOnLine*, vol. 50, no. 1, pp. 3953–3958, Jul. 2017.

[21] Z. Dong, T. Bao, M. Zheng, X. Yang, L. Song, and Y. Mao, "Heading control of unmanned marine vehicles based on an improved robust adaptive fuzzy neural network control algorithm," *IEEE Access*, vol. 7, pp. 9704–9713, 2019.

[22] R. Font and J. García-Peláez, "On a submarine hovering system based on blowing and venting of ballast tanks," *Ocean Eng.*, vol. 72, pp. 441–447, Nov. 2013.

[23] F. Min, G. Pan, and X. Xu, "Modeling of autonomous underwater vehicles with multi-propellers based on maximum likelihood method," *J. Mar. Sci. Eng.*, vol. 8, no. 6, p. 407, Jun. 2020.

[24] L. Wen-Tao and G. Tong, "Research on control strategy of a hovering-type AUV," *Ocean Eng.*, vol. 29, no. 1, pp. 75–81, 2011.

[25] T. I. Fossen, *Guidance and Control of Ocean Vehicles*. London, U.K.: Wiley, 1994.

[26] J. García, D. M. Ovalle, and F. Periago. (2009). *Optimal Control Design for the Nonlinear Manoeuvrability of a Submarine*. [Online]. Available: https://www.researchgate.net/publication/228909707
[27] L. Pugi, M. Pagliai, and B. Allotta, "A robust propulsion layout for underwater vehicles with enhanced manoeuvrability and reliability features," *Proc. Inst. Mech. Eng., Part M, J. Eng. Maritime Environ.*, vol. 232, no. 3, pp. 358–376, Aug. 2018.
[28] M. Caccia, G. Bruzzone, and G. Veruggio, "Hovering and altitude control for open-frame UUVs," in *Proc. IEEE Int. Conf. Robot. Automat.*, Detroit, MI, USA, Feb. 1999, pp. 72–77.

FEIYAN MIN received the B.E. degree in automation and the M.S. and Ph.D. degrees in navigation, guidance, and control from the Harbin Institute of Technology, Harbin, China, in 2003, 2005, and 2009, respectively.

From December 2009 to December 2017, he was an Engineer with the Navigation Instruments Institute of Tianjin, China Shipbuilding Industry Corporation (CSIC). Since June 2017, he has been with the College of Information Science and Technology, Jinan University, Guangzhou, China. His research interests include underwater vehicle and industrial robot.

FANGHONG YANG was born in Yangjiang, Guangdong, China, in 1996. He received the bachelor's degree in electronic science and technology from the Xi'an University of Posts and Telecommunications, Xi'an, Shaanxi, in 2019. He is currently pursuing the master's degree in circuits and systems with Jinan University, Guangdong.

His research interest includes robot application and action analysis.

GAO WANG received the master's and Ph.D. degrees from SCUT. He is currently an Assistant Professor with the Department of Electronic Engineering, College of Information Science and Technology, Jinan University. He has 20 years of combined academic and industrial experience. His research interests include collaborative robotics, flexible manufacturing, and defects detection and fault diagnosis in manufacturing processes.

XINYU YE received the B.S. degree in automation and the M.S. degree in aeronautical engineering from Beihang University, Beijing, China, in 2011 and 2014, respectively.

He is currently working as an Engineer with the Navigation Instruments Institute of Tianjin. His research interests include automation steering of vessels and motion control of underwater vehicles.